令和５年度修士学位論文

A High-Speed Stereo Tracking System for Remote One-Man Operation

M213684 WANG JIAHUA

August 18, 2023

Thesis submitted to the Department of Advanced Science, Graduate School of Engineering, Hiroshima University in partial fulfillment of the requirements for the degree of Master of Engineering.

Contents

List of Figures

List of Tables

1 Introduction

Since the onset of the coronavirus disease pandemic in 2019, various policies in different countries [1] have facilitated telecommuting as a popular work option because many people have been unable to attend their workplaces. Acquiring remote visual information and performing remote control are essential when a geographical location is distant or inaccessible. Therefore, remote monitoring systems can solve numerous problems in industry and other areas.

High-speed vision [2] refers to the acquisition and processing of images using high-frame-rate cameras. A series of processing steps starting from the time of image capture can run in real time at a speed of hundreds to thousands of frames per second (fps), allowing one to observe rapid changes in a target in real time. Unlike typical cameras that operate at tens of frames per second, high-speed vision facilitates the observation of the vibration frequency of objects [3] or reproduction of sound [4].

A camera with a fixed viewing angle is inadequate to satisfy high-speed requirements for processing data with a wide field of view. Therefore, components that can control a camera ' s perspective are required. Traditional methods typically use a gimbal to drive the transformation of the angle of view of a Pan-tilt-zoom (PTZ) camera. However, gimbal-based cameras have various disadvantages. First, based on the limitation of motor speed, such cameras cannot achieve a high rotational speed. Additionally, rotation requires a camera to rotate concurrently, resulting in vibration and degraded image quality.

A galvanometer mirror is an optical scanner that is highly valued for its ability to achieve high-speed, high-precision, and reliable performance. Typically, such a device utilizes two mirrors to control and manipulate the viewing angle, which facilitates adjustment of the viewing angle at a remarkably rapid pace with exceptional precision and stability. Based on their unique features, galvanometer mirrors are frequently paired with high-speed cameras in various applications. This combination facilitates the capture of fast-moving objects with high accuracy and detail, and is useful in fields such as scientific research, industrial manufacturing, and security surveillance. Aoyama et al. [5] proposed a view expansion system for photomicroscopy using the observing point movement of a Galvano mirror, which fully demonstrates that the galvanometer mirrors can also be applied to precision instruments such as microscopes. A galvanometer mirror is an essential tool in numerous settings where the precise and rapid scanning of a large area is required.

Active vision [6] is an area of computer vision that is commonly considered

in the fields of object detection and visual tracking. In particular, researchers such as Jiang et al. [7] have successfully utilized galvanometer reflections to capture images and rapidly detect the locations of objects at a remarkable speed of 500 fps. To achieve high-speed object tracking, they employed a galvanometer that could be precisely controlled to monitor object movement. Similarly, Hu et al. [8] expanded this approach by combining panoramic and galvanometer cameras. A panoramic camera was used to detect targets using deep learning and a galvanometer camera rapidly switched between multiple targets at 500 fps. By using this technique, multiple targets can be tracked effectively with high precision and efficiency.

Additionally, the capabilities of a single camera with a rotatable viewing angle are limited. When cameras are installed in multiple locations to form a camera network, multi-angle images can be used to collect the three-dimensional spatial information associated with an observed target to achieve more accurate tracking [9] or 3D reconstruction based on visual information [10].

In this study, we developed a system capable of remotely controlling multiple galvanometer-based camera systems in different locations simultaneously to observe the same location as a human binocular auto-focus. We verified the effectiveness of our remote tracking system through tracking experiments. In a realistic experiment, tracking with viewing angle calculation was able to match the camera capture speed of 500 frames per second (fps). Even after adding a tracking algorithm based on template matching [11], the proposed system could still reach at least 200 fps. Users can control remote cameras to observe a target from multiple perspectives with a delay that is undetectable by humans.

In the next sections, I will detail our system and explain the hardware in Section 2, and explain the specific algorithms in Section 3. In Section 4 we demonstrate the performance of our system through some experiments. Finally, in Section 5 we summarize the conclusions and discuss future improvement directions.

2 Remote Multi-Camera Tracking System

2.1 Concept

When observing a target, humans can accurately maintain binocular vision, regardless of the distance to the target. For bionic eyes composed of gimbal or galvanometer mirrors, it is exceedingly difficult to control multiple cameras to focus to the same target simultaneously. In certain conventional methods, all angles are typically traversed to locate similar targets, but searching is time consuming, particularly when using a telephoto lens to observe distant targets, which requires numerous traversals and image-matching operations. Additionally, this process requires separate operators for each camera like figure 1.

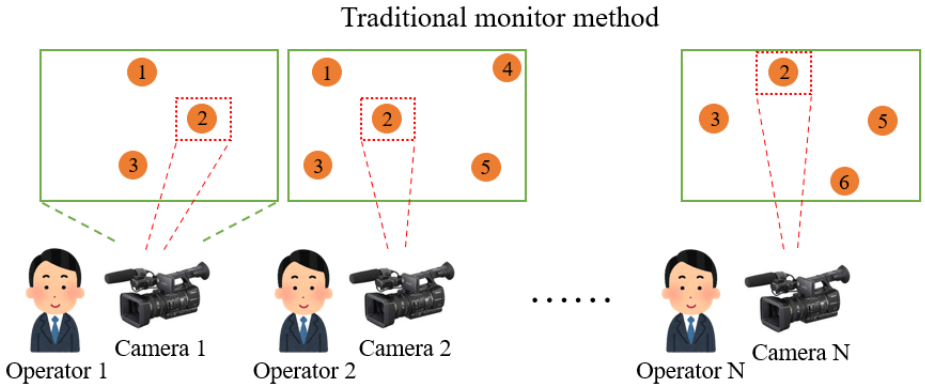

Figure 1: Tracking using the traditional method

Therefore, in this study, we leveraged the three-dimensional relationships between different galvanometer systems to calculate the angles required to find a target, which significantly reduces search time and manpower requirements. Figure 2 illustrate a concept that contrasts the proposed system with the traditional method of monitoring a target.

In our method, we select a single camera system as the master camera system and the other cameras are considered as slave camera systems. After receiving a search command, each slave camera system calculates the current line of sight of the master camera system. In epipolar geometry [12], we refer to this line of sight as the epipolar line or epiline [13]. The slave cameras then search for a target along the epiline, which significantly reduces the search range. A reduced search range allows the system to avoid tracking incorrect targets with similar appearances during the search process, thereby improving search accuracy. After finding the target, the system can obtain constant depth information to begin follow-up tracking operations. For ease

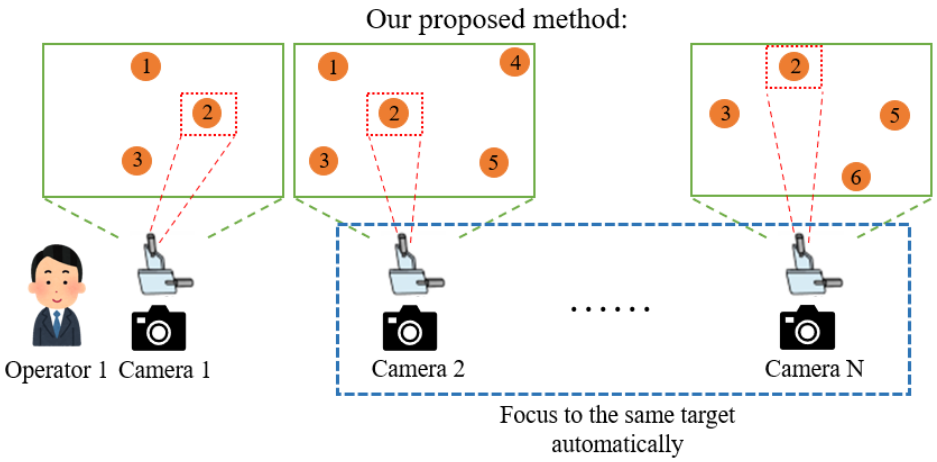

Figure 2: Tracking using the proposed method

of use in many different situations, we made a graphical interface, which allows adjustment of various parameters in the experiment. The details are shown in Figure 3.

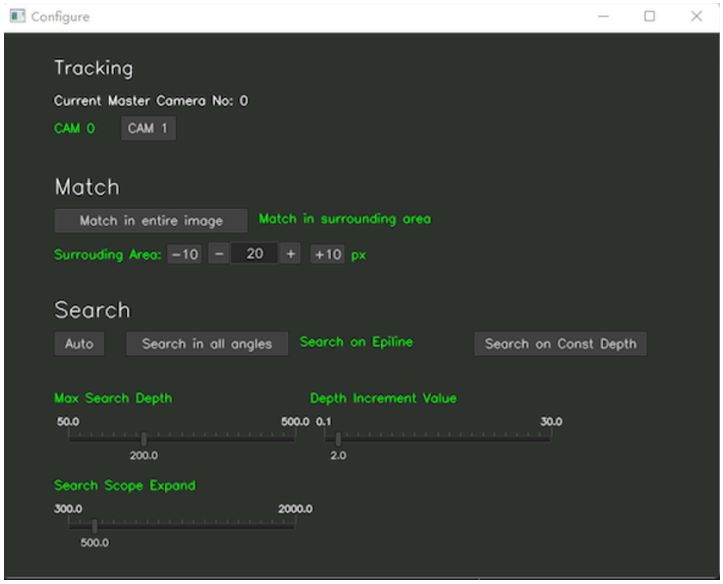

Figure 3: User interface of the proposed system

A multiview tracking system based on 3D information enables cameras in multiple locations to be operated by only a single operator and enables that operator to observe the appearance of the same target from multiple viewing angles simultaneously. This method can be applied in various scenarios.

(1) Remote monitoring of factory equipment

In factories, it is often necessary to observe equipment from multiple directions to determine whether it is operating normally. However, in a factory, there are typically multiple devices with the same appearance. It is easy to track other targets with similar appearances mistakenly when traditional methods are used to perform traversal searches from multiple perspectives. Because our method searches along the master camera ' s line of sight, it reduces the search range and avoids most false targets with similar appearances. This enables a single operator to easily and accurately monitor the factories' equipment.

(2) Target tracking in sports games

In sports games such as football, one often wishes to track the same player or ball in multiple positions. Traditional methods require an operator to track each camera. In contrast, our method enables a single operator to simultaneously control all of the cameras and track them.

(3) Observing extremely distant targets from multiple perspectives

To observe extremely distant targets, our method reduces the search range to the master camera ' s line of sight, in contrast to a traditional traversal search, which requires a larger search area. This system enables the originally enormous workload to be accomplished by a single individual.

2.2 System Configuration

The proposed remote tracking system uses a stand to carry two galvanometer systems, each of which consists of a pair of mirrors and DMK 37BUX287 camera with a 35 mm F/1.9 lens. We used a PC with an Intel(R) Core(TM) i9-12900K 3.19 GHz CPU, 64 GB of RAM, and Windows 11 OS for processing. Figure 4 presents the system equipment. In actual use, one of the cameras can be selected as the master camera in the user interface. In this study, we simply used the camera on the left in Figure 4 as the master camera.

To simplify camera calibration, we set the two galvanometer systems at the same level and adjusted their orientation to be consistent. We assumed that the positions of the two galvanometer systems were the same on the Y and Z axes, and that there was only a difference in the X axis, which is the physical distance between the two galvanometer systems. We denote this distance as D. For orientation, we assumed that both cameras had the same orientation. Therefore, when the pan-tilt angles of the two mirrors are identical, the lines of sight of the two galvanometer systems are parallel.
Because the depth of the target is unknown, in an actual epiline search, the galvanometer mirror of the slave camera continues to search forward along the epiline of the master camera starting from its position at a depth of zero. Therefore, a maximum search depth must be defined and gradually increased for each traversal. We designed these values to be modifiable to facilitate tracking of both distant and near targets. Users can set these values through the system ' s user interface.

Besides, figures 5 to 10 and tables 1 to 3 introduce the hardware used in this system.

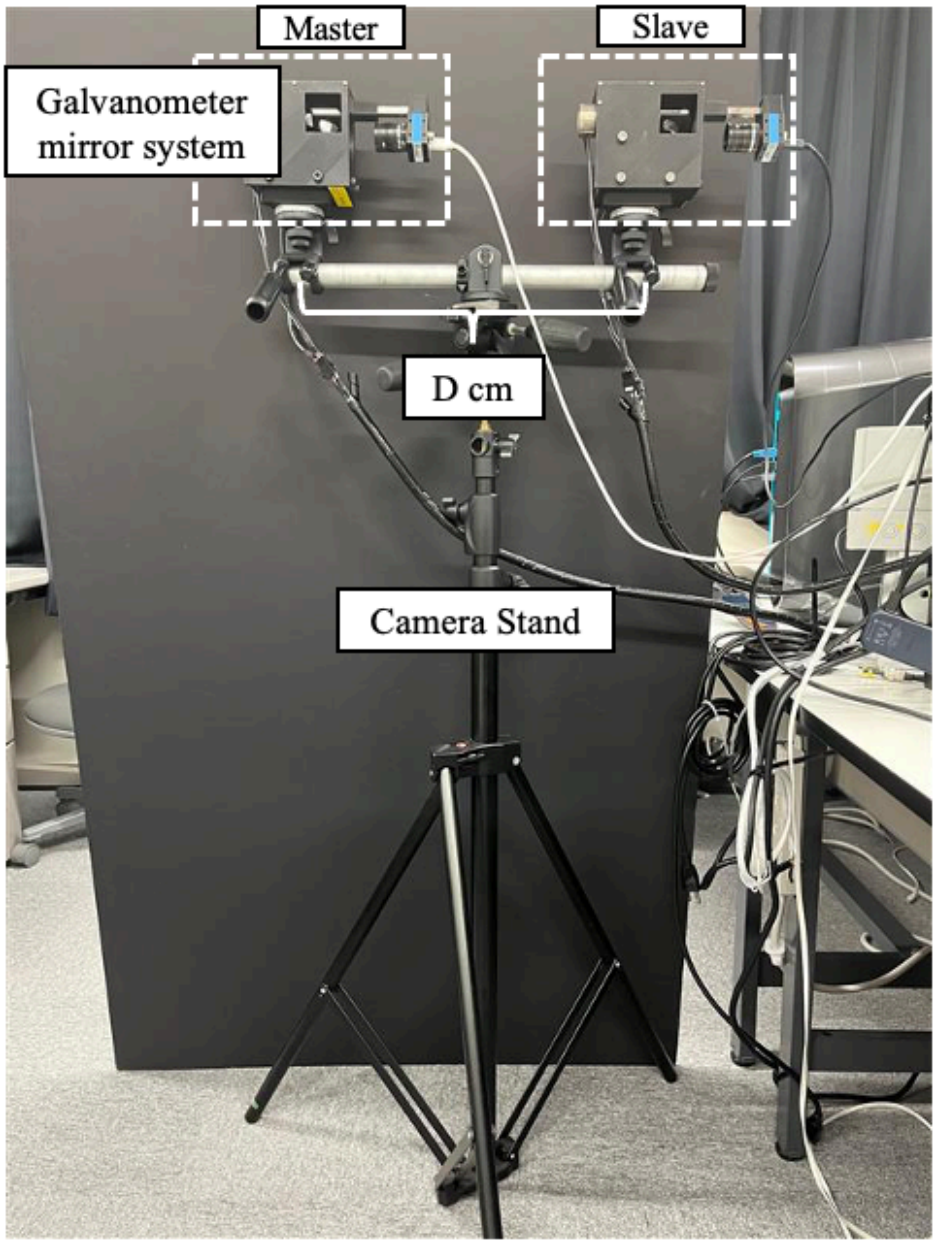

Figure 4: System configuration

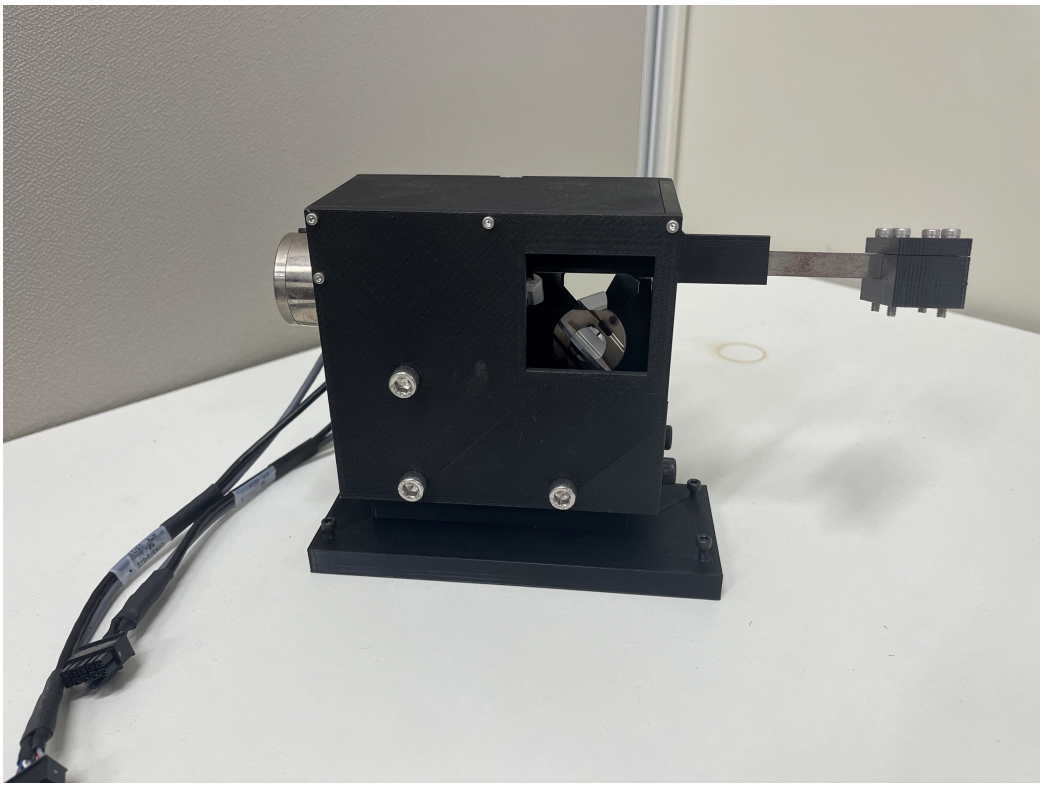

Figure 5: The front of galvanomirror

Mirror angle	$\pm$ 20°
Settling time	350 µs
Two-axis distance	15 mm

Table 1: Specification of galvanometer mirror

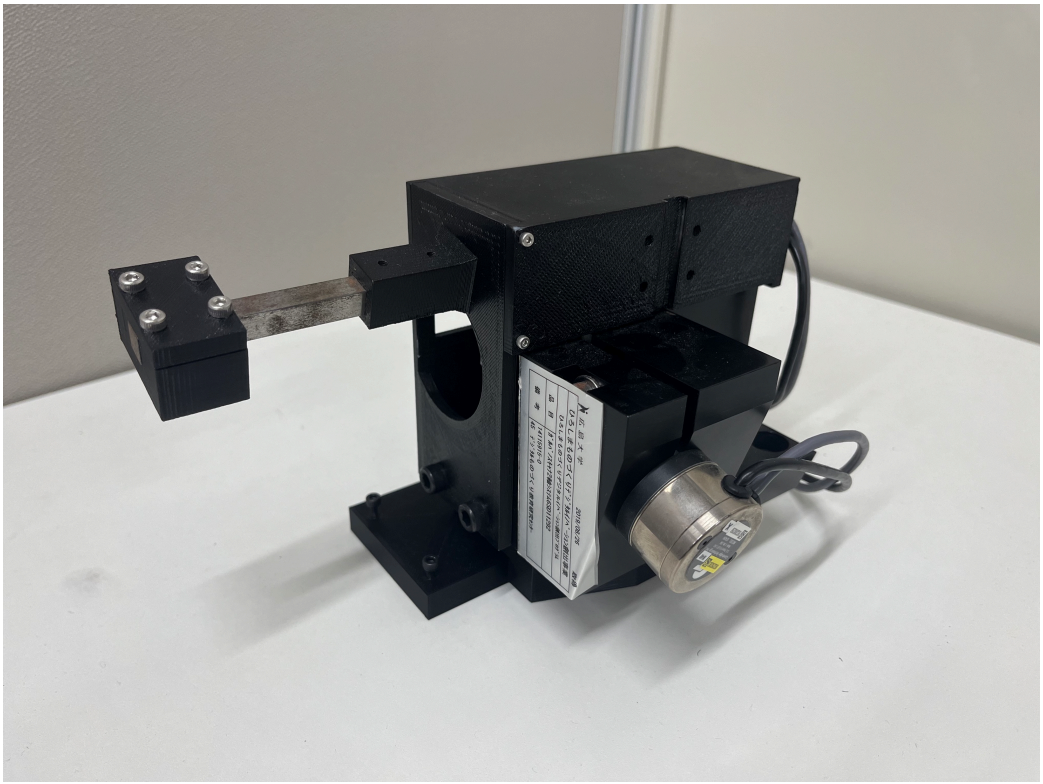

Figure 6: The rear of galvanomirror

Figure 7: Lens of the camera

Zoom	35 mm
Aperture	1:1.9

Table 2: Specification of the lens

Figure 8: High speed camera of the system

Model	Imaging Source DFK 37BUX287
Sensor specification	Sony IMX287
Resolution	720×540 pixel
Pixel size	H: 3.45 µm, V: 3.45 µm
Frame rate	539 fps
Exposure Time	1/1000000 sec
Lens mount	C/CS

Table 3: Specification of the camera

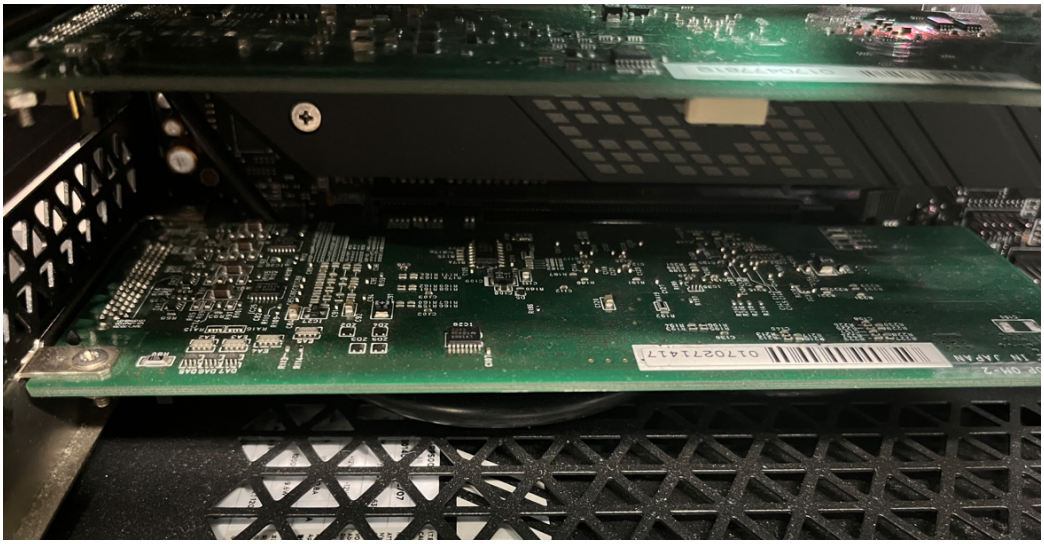

Figure 9: ADDA board of the system

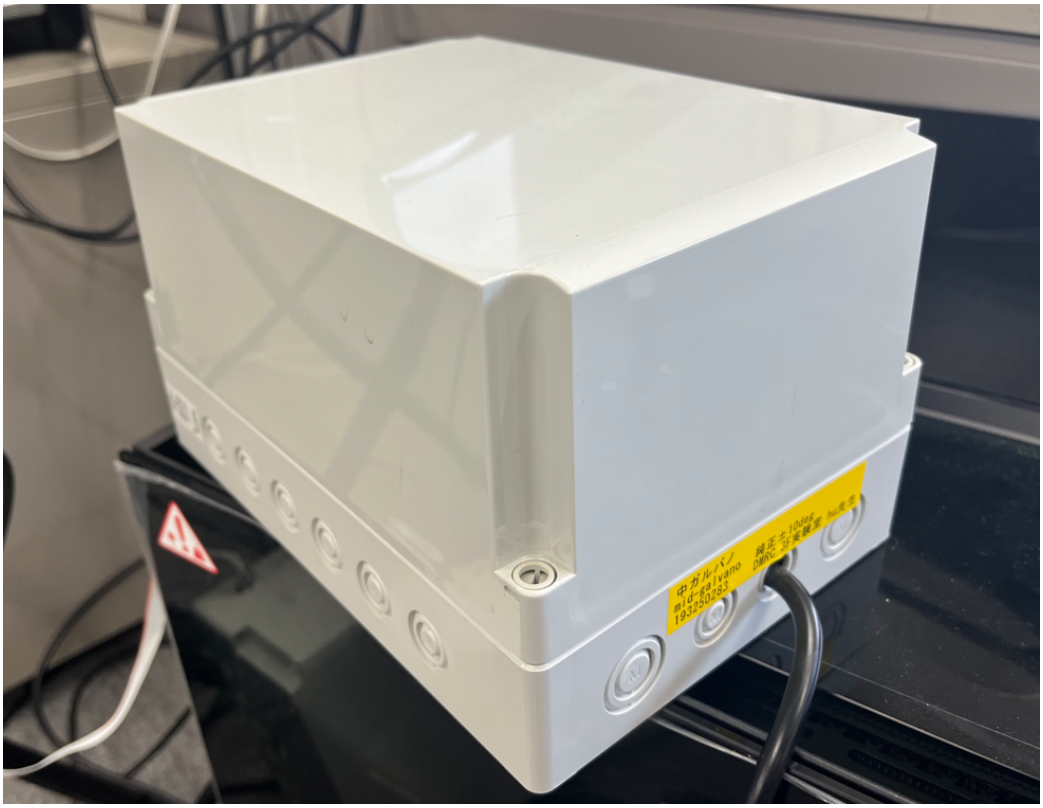

Figure 10: ADDA convertor of the system

3 Algorithms

In this study, to achieve remote multiview monitoring with single-user operation, the following algorithms were adopted.

3.1 Epiline Search Algorithm

Compared to a gimbal-based camera, the imaging path and mirror reflection relationships of a galvanometer system are more complicated. Therefore, they are difficult to calibrate. Wissel et al. [14] proposed a data-driven calibration method that requires large amounts of data. Li et al. [15] proposed a method capable of calibrating a galvanometer system as a calibration method for a reflective galvanometer bionic eye. This method virtualizes the galvanometer into a camera model and projects three-dimensional spatial points onto the control voltage parameter space of the galvanometer, and has high precision. Our system uses this study to map the master camera ' s line of sight and galvanometer angle into the coordinate systems of different galvanometer systems.

Specifically, we use Eqs. (1) and (2) to convert the angle of the mirror into a point in a coordinate system. These equations represent the relationships between the mirror angles and corresponding three-dimensional coordinate values. Eq. (2) cannot directly obtain coordinate values, but can obtain the relationships among X, Y, and Z. Therefore, we must use the assumed Z value to calculate X and Y. During the epiline search, we first set the Z value to zero and then slightly increase it to search additional positions along the epiline gradually. The value of e in Eq. (2) is the distance between the two mirrors in the galvanometer mirror system.

$$\begin{cases} \theta_{\mathrm{t}} = \frac{1}{2}\arctan\frac{y_g}{z_g} \\ \theta_{\mathrm{p}} = \frac{1}{2}\arctan\frac{x_g}{z_g\sec 2\theta_{\mathrm{t}}+e}. \end{cases} \tag{1}$$

$$\begin{cases} y_g = z_g\tan\left(2\theta_{\mathrm{t}}\right) \\ x_g = \tan\left(2\theta_{\mathrm{p}}\right)\left(z_g\sec\left(2\theta_{\mathrm{t}}\right)+e\right). \end{cases} \tag{2}$$

Figures 11 and 12 illustrate the process of an epiline search. First, the operator controls the mirror of the master camera system to select a region of interest (ROI) as a target and all camera systems save the selected ROI. Because the Y and Z axes of the two camera systems in the considered system are identical, there is only a distance D along the X axis to consider and the camera systems have the same orientation when the galvanometer angle is the same. As long as the coordinate system X of the slave camera system

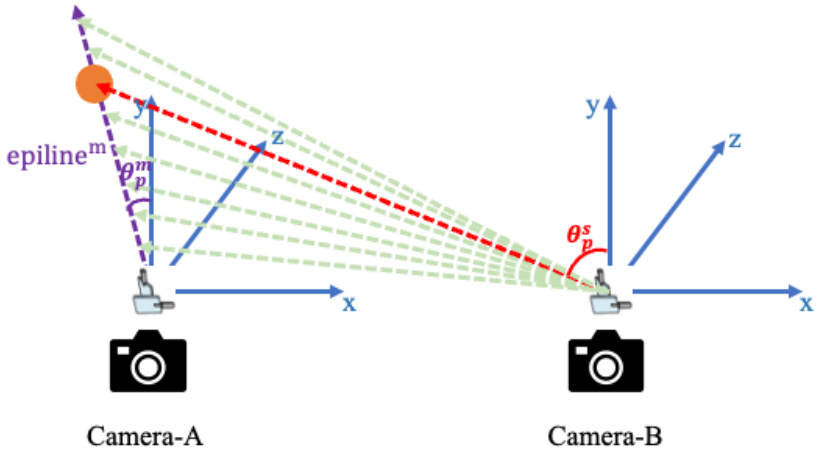

Figure 11: Conversition of coordinates and angles during an epiline search

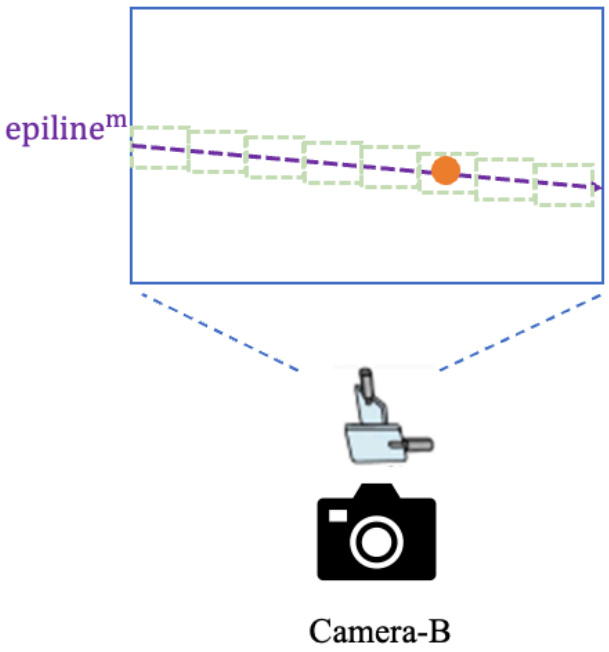

Figure 12: Epiline in the frame of a slave camera

adds the distance D to its axis, the two camera systems can share the same coordinate system. Subsequently, we consider an initial depth, which is the value of the Z axis, and replace it with the mirror angles θ_p and θ_t of the master camera system in Eq. (2) to calculate the X and Y values. We then obtain the complete 3D coordinates of a hypothetical target. Subsequently, we substitute these 3D coordinates into Eq. (1) to calculate the angles θ_p and θ_t to which the slave camera system should rotate. Finally, the mirror of the slave camera system must be controlled to rotate to the corresponding angle to search for the target. The search process begins from a position where the depth is one and proceeds to the maximum search depth defined by the user.

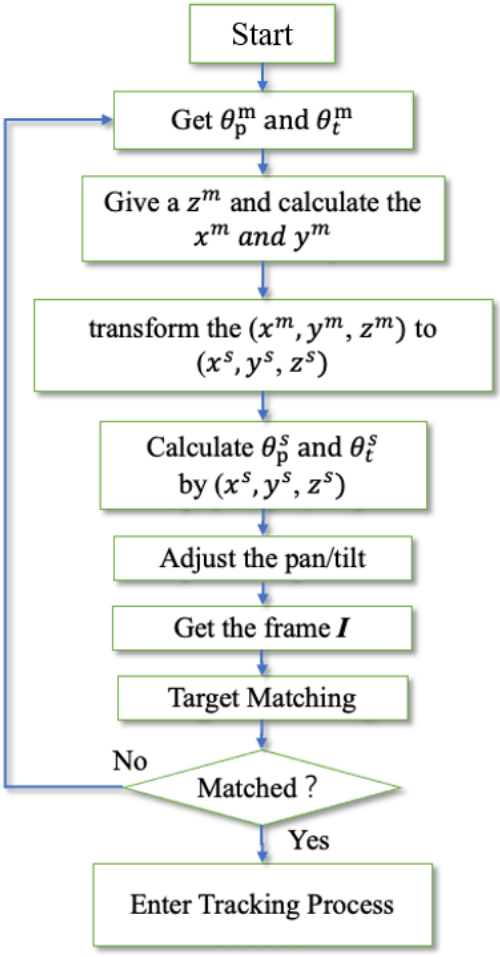

Figure 13: Flow chart of the epiline search

Figure 13 illustrates the epiline search algorithm described above using

a flowchart, where the superscript S denotes the slave and superscript M denotes the master.

In each search, we perform template matching based on the normalized sum of squared differences to find the target ROI in the camera frame. Equation (3) defines the principle of template matching, where the sum of the squared differences between the template and input image is computed at each possible position of the template within the input image.

$$R(x, y) = \sum_{u,v} [T(u, v) - I(x + u, y + v)]^2 \tag{3}$$

In this equation, R(x,y) is an output image containing the correlation coefficients between the template T and input image I, (x, y) is the pixel location of the top-left corner of the current window considered in I, and (u,v) is the pixel location of the current pixel considered in template T. In the output image R, higher values indicate better matching between the template and input image, meaning the location of the maximum value of R(x,y) may correspond to the position of the target. Therefore, after searching all frames along the epiline, we can obtain the depth value of the target by selecting the maximum value among all values of R(x,y).

3.2 Real-Time Multi-Camera Tracking Algorithm

We implemented tracking functions based on user operations such as allowing users to operate the galvanometer of one camera freely while the other cameras maintain their own perspectives, focusing on the same position monitored by the user in real time. The geometric principle of this function is shown in Figure 14.

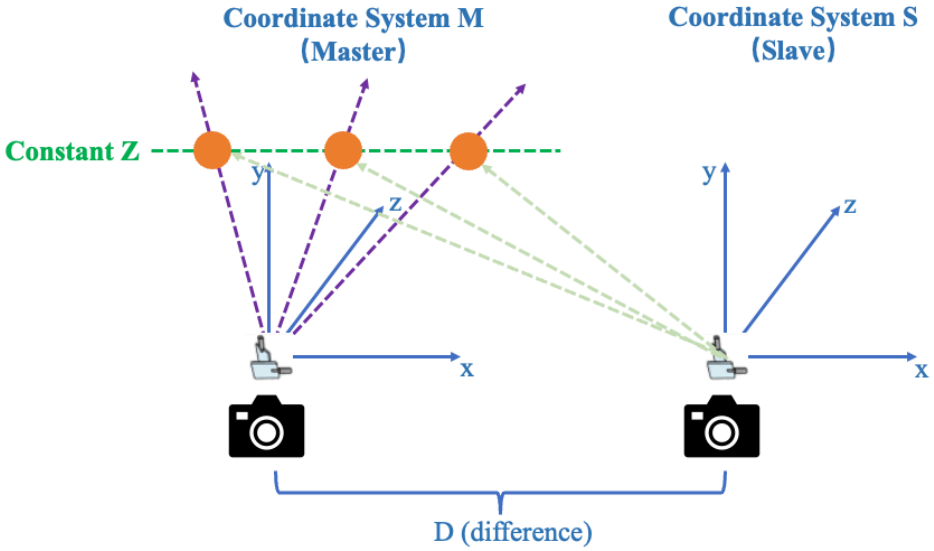

Figure 14: Geometry of real-time tracking with constant depth

When using the epiline search process, the Z axis of the target must be determined when transforming the camera coordinate system into the camera angle. Therefore, we assume that when a user actively controls the galvanometer mirrors for tracking, the Z-axis value of the position that the user wishes to monitor does not change significantly relative to the camera (e.g., using a camera at a greater distance to monitor a certain area), meaning we only need to consider a constant Z axis value.

In this scenario, the Z is determined and the angles of the two mirrors in the master camera are known. By using the Eq. (2) provided in the previous context, we are able to calculate the values of the target's coordinate in the master camera's 3-D coordinate system.

$$\begin{cases} y^{master} = z_{constant} \tan\left(2\theta_{\mathrm{t}}^{master}\right) \\ x^{master} = \tan\left(2\theta_{\mathrm{p}}^{master}\right)\left(z_{constant} \sec\left(2\theta_{\mathrm{t}}^{master}\right) + e\right). \end{cases} \tag{4}$$

Subsequently, through coordinate axis transformation, we can obtain the target's coordinate in the slave camera's coordinate system.

$$\begin{cases} x^{slave} = x^{master} - D \\ \quad y^{slave} = y^{master} \end{cases} \tag{5}$$

Finally, we utilize Eq. (1) to calculate the angle by which the slave camera mirrors should be rotated.

$$\begin{cases} \theta_{\mathrm{t}}^{slave} = \frac{1}{2} \arctan \frac{y^{slave}}{z_g} \\ \theta_{\mathrm{p}}^{slave} = \frac{1}{2} \arctan \frac{x^{slave}}{z^{constant} \sec 2\theta_{\mathrm{t}}^{slave} + e}. \end{cases} \tag{6}$$

It is worth noting that this method does not involve image matching. Instead, it solely relies on utilizing three-dimensional spatial information and the angles of the mirrors while the user controls the line of sight using the master camera. Therefore, the computational time is significantly low, with actual speed measurement results ranging between 0.8 to 1.2 microseconds. This implies that the proposed system can maintain real-time calculations even when using high-speed cameras with frame rates as high as 1,000,000 fps.

4 Experiments

4.1 Evaluation of Tracking Capabilities

We conducted experiments to determine whether the slave cameras in the proposed tracking system could successfully track a target. The setting of the experimental scene is shown in the figure 15.

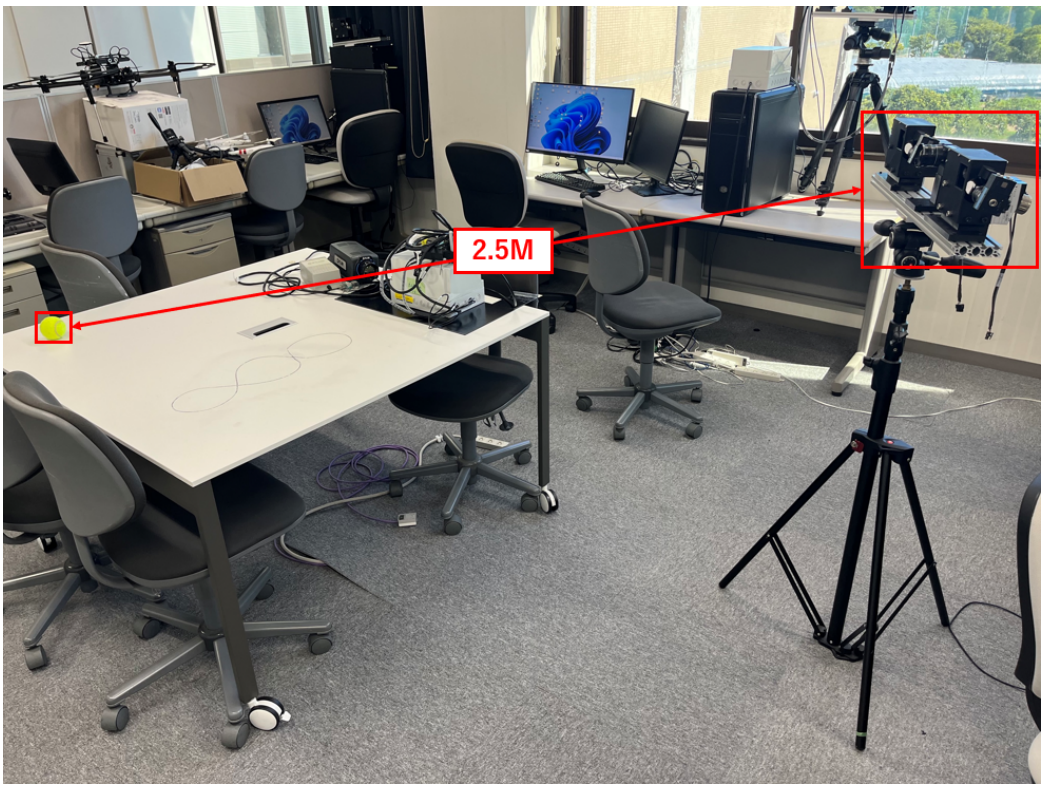

Figure 15: Experiment setting of tracking capability evaluation

In these experiments, the target size was 50 × 50 px and the matching range was 20 px. Figure 16 presents a chart of the observed similarity changes, which were calculated by performing template matching in the slave camera frames after tracking began.

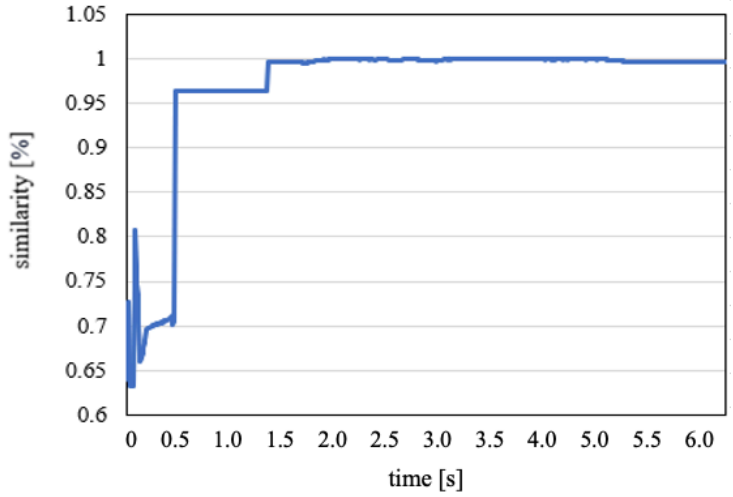

Figure 16: Similarity changes during tracking

We can see that in the first 0.5 s the similarity is very low due to the slave camera undergoing a search process. After some fluctuations, it reaches approximately 96% around 0.5 s and stabilizes. At around 1.5 s, we start controlling the angle of the master camera to observe other positions. As the background in the camera frame is relatively simple at this point, the similarity is increased to nearly 99%.

We also did some experiments to observe the camera frames during the search process, six pairs of images from the epiline search process are presented in Figure 17. The left side of each pair of images is an image from the master camera and the right side is an image from the slave camera. In the first four images, the slave camera searches the epipolar line from right to left, but the target cannot be observed in these images. Therefore, the similarity is low. The target can be observed in the fifth image from the slave camera, but it is not in the center because the epiline search has not yet been completed. In the sixth image, both cameras are locked onto the target and the matching similarity reaches 94%. This experiment demonstrates that the proposed system can successfully search for a target on the epiline and then assist a user in performing tracking.

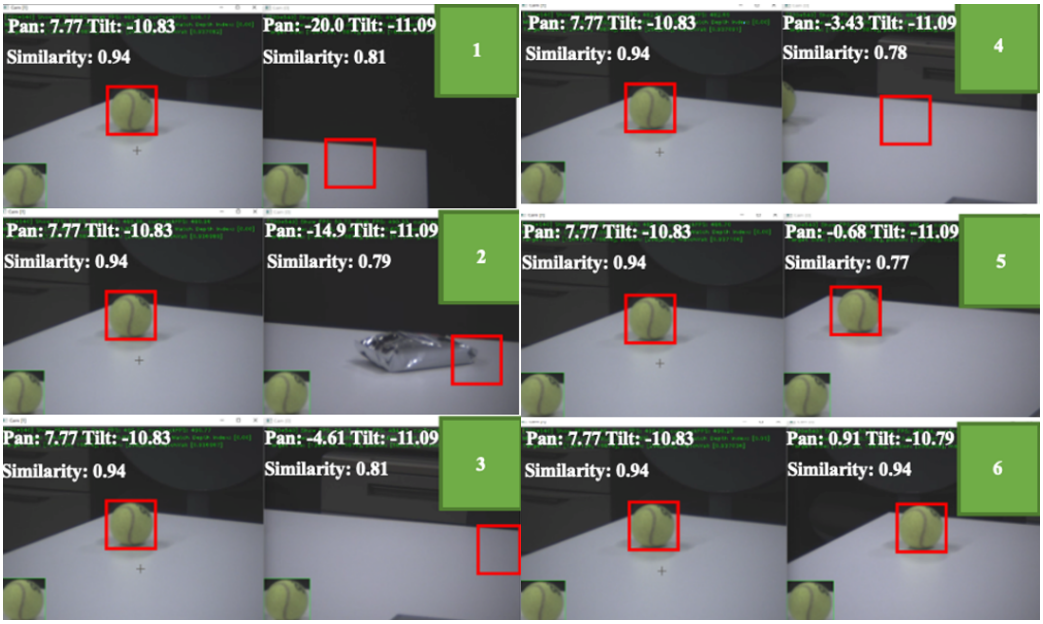

Figure 17: Frames during an epiline search prior to tracking

4.2 Real-time Stereo Tracking for Remote One-Man Operation

To investigate frame rate changes during tracking, we conducted experiments in which we set the target size to 50 * 50 px and the matching range to 20 px. Figure 18 presents the results of these experiment, where one can observe the FPS changes in both master and slave cameras during the tracking process.

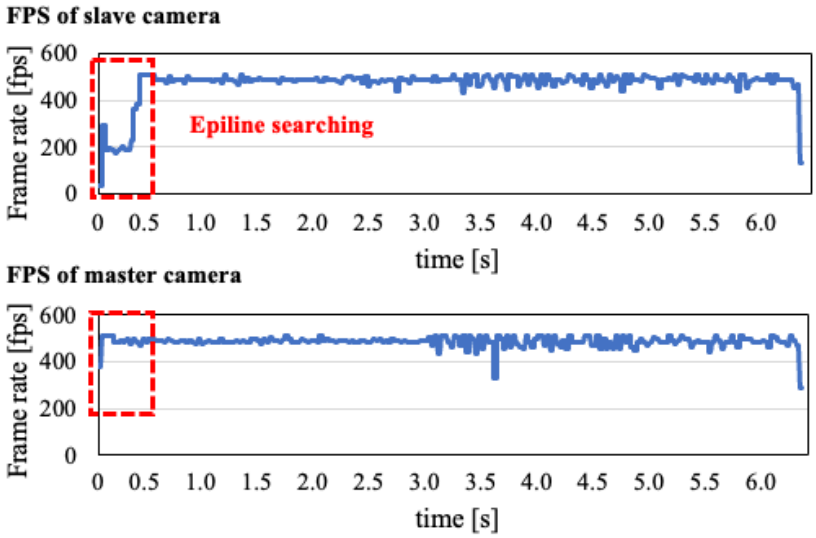

Figure 18: FPS changing during tracking

Notably, during the initial 0.5 seconds, the frame rate of the slave camera remains at approximately 200 fps, reflecting the load imposed by the epiline search process. However, as the tracking process commences, the FPS of the slave camera experiences a significant boost, reaching 500 fps. This value matches the hardware limit of the camera used and aligns with the frame rate of the master camera. This observation indicates the efficiency of our system in handling the tracking process without any delay. Furthermore, we conducted additional investigations by considering various target sizes to explore their impact on the frame rate. Surprisingly, we found that even with larger target sizes, the system effectively maintained a stable frame rate of 500 fps. The reason behind this impressive performance lies in our optimization approach. Once the epiline search process is completed, the system only needs to match the template in the central regions of the captured images, rather than the entire images. As a result, the time required for template matching is significantly reduced, enabling the system to handle larger targets seamlessly without sacrificing performance.

The outcomes of this comprehensive experiment offer compelling evidence that our proposed system can flawlessly execute simultaneous tracking using 500 fps cameras without any noticeable delay. This finding underscores the effectiveness and reliability of our system in maintaining a stable frame rate during tracking operations. The ability to consistently achieve a high frame rate is of paramount importance in ensuring the accuracy and dependability of the tracking process, making our system a robust and dependable solution for a wide range of real-world applications.

4.3 Evaluation of Tracking Accuracy

Experiments were conducted to test the accuracy of the slave camera angles when a user was performing real-time tracking. Ideally, when the user operates the master camera for tracking, the system should ensure that the object at the focal point of the master camera remains in the center of the slave camera display if the depth of the target does not change significantly. We tracked 3 targets at different distance and the setting of the experimental scene is shown in the figure 19.

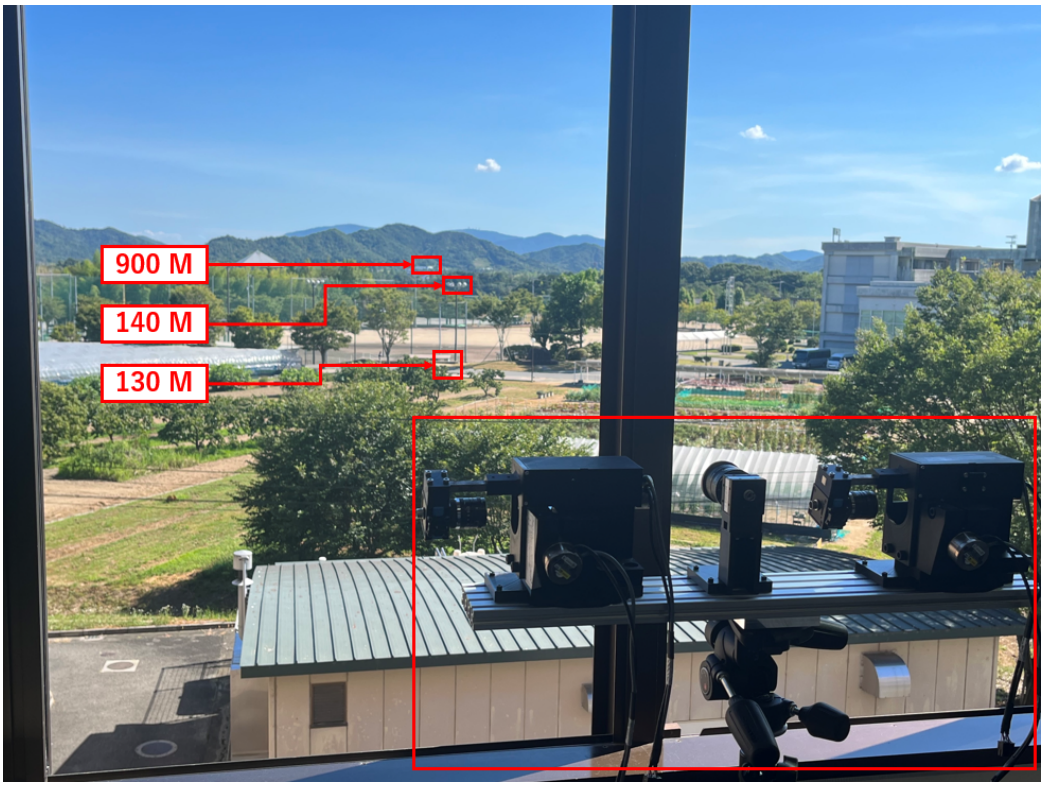

Figure 19: Experiment setting of tracking accuracy evaluation

Figure 20 presents the relationship between the pan angles of the master and slave cameras during tracking. One can see that the angles of the slave camera change responsively as the angles of the master camera change. The tilt angles of the slave camera cannot be clearly found in the figure, because master-tilt and slave-tilt are the same line due to the same Y and Z axes of the camera positions. Figure 21 presents the tracking performance for 3 distant targets. The left side of each pair of images is an image from the master camera and the right side is an image from the slave camera. One can see that the targets in the slave camera images are always in the center

of each image, which demonstrates that our system can accurately center the target selected by the user in its slave camera images. Even if the user adjusts the angles of the master camera, a slave camera can monitor the same position in real time without any offset.

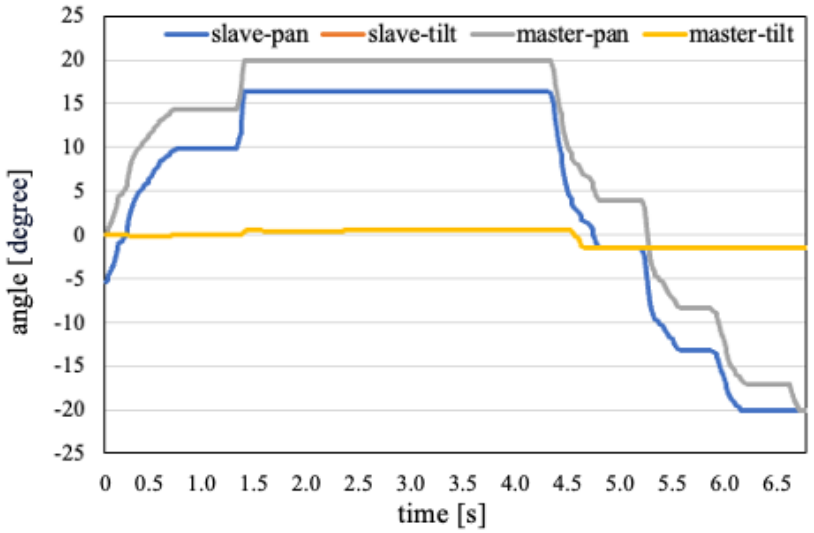

Figure 20: Changes in pan-tilt during tracking

Figure 21: Tracking images of distant scenery

5 Conclusion

In this study, two high-speed cameras with galvanometer mirrors are used to develop a high-speed stereo tracking system. By leveraging the 3D relationships between cameras, all cameras can be controlled to focus to the same position rapidly with reduced manpower. We proposed a novel scheme to address the challenge of rapidly searching for and tracking targets from multiple perspectives in high-speed vision. Given our aging society and continued industrial development, we hope to reduce the manpower required for complex tasks and enable remote, multi-perspective tracking.

However, there is scope for further improvement. To simplify the calibration process, we placed two cameras on the same Y and Z axes, and adjusted their orientations for consistency. In future work, we aim to use the galvanometer calibration method proposed by Li et al. to improve the effectiveness of this system for more complex camera networks. Additionally, we intend to add more cameras to realize a larger camera network and perform stereo tracking.

6 Acknowledgments

I am honored to express my feelings in this thesis. During my master's study, I got a great deal of assistance from many people.

First, I want to express my gratitude to my advisor, Prof. Idaku Ishii, who possesses a wealth of knowledge in the field of high-speed vision. His valuable insights and suggestions have been instrumental in my research, allowing me to contemplate and improve my study from various perspectives. Also, Prof. Takaki and Prof. Chikaraishi who are the associate professors gave me some good advice.

I would like to extend thanks to Asst. Prof. Kohei Shimasaki from our laboratory, as he provided me with abundant technical support and advice throughout the research process. I am also deeply appreciative of designated Asst. Prof. Shaopeng Hu and Feiyue Wang, along with Doctoral student Qing Li, for their help. Their valuable opinions have helped me resolve many doubts and questions.

Additionally, as a student in the TAOYAKA Program, I would like to express my gratitude to all of the members of TAOYAKA. This program has given me a deeper understanding of Japan as a country and how my research can help people.

Finally, I want to express my heartfelt appreciation to my parents and sister, who have steadfastly supported all my decisions.

Lastly, I am grateful to all of the members of Smart Robotics Laboratory and all my friends who have been by my side, adding vibrant colors to my life.

Augest 18, 2024
WANG JIAHUA

Bibliography

[1] Thomas Hale, Noam Angrist, Rafael Goldszmidt, Beatriz Kira, Anna Petherick, Toby Phillips, Samuel Webster, Emily Cameron-Blake, Laura Hallas, Saptarshi Majumdar, et al. A global panel database of pandemic policies (oxford covid-19 government response tracker). *Nature human behaviour*, 5(4):529–538, 2021.

[2] Yoshihiro Watanabe, Hiromasa Oku, and Masatoshi Ishikawa. Architectures and applications of high-speed vision. *Optical Review*, 21:875–882, 2014.

[3] Qican Zhang and Xianyu Su. High-speed optical measurement for the drumhead vibration. *Optics express*, 13(8):3110–3116, 2005.

[4] Kohei Shimasaki, Tomoaki Okamura, Mingjun Jiang, Takeshi Takaki, and Idaku Ishii. Real-time high-speed vision-based vibration spectrum imaging. In *2019 IEEE/SICE International Symposium on System Integration (SII)*, pages 474–477. IEEE, 2019.

[5] Tadayoshi Aoyama, Mamoru Kaneishi, Takeshi Takaki, and Idaku Ishii. View expansion system for microscope photography based on viewpoint movement using galvano mirror. In *2017 IEEE/RSJ International Conference on Intelligent Robots and Systems (IROS)*, pages 1140–1145, 2017.

[6] John Aloimonos, Isaac Weiss, and Amit Bandyopadhyay. Active vision. *International journal of computer vision*, 1:333–356, 1988.

[7] Mingjun Jiang, Kohei Shimasaki, Shaopeng Hu, Taku Senoo, and Idaku Ishii. A 500-fps pan-tilt tracking system with deep-learning-based object detection. *IEEE Robotics and Automation Letters*, 6(2):691–698, 2021.

[8] Shaopeng Hu, Kohei Shimasaki, Mingjun Jiang, Taku Senoo, and Idaku Ishii. A simultaneous multi-object zooming system using an ultrafast pan-tilt camera. *IEEE Sensors Journal*, 21(7):9436–9448, 2021.

[9] Y. Nakabo, I. Ishi, and M. Ishikawa. 3d tracking using two high-speed vision systems. In *IEEE/RSJ International Conference on Intelligent Robots and Systems*, volume 1, pages 360–365 vol.1, 2002.

[10] E. Mouragnon, M. Lhuillier, M. Dhome, F. Dekeyser, and P. Sayd. Real time localization and 3d reconstruction. In *2006 IEEE Computer Society*

Conference on Computer Vision and Pattern Recognition (CVPR'06), volume 1, pages 363–370, 2006.

[11] Roberto Brunelli. *Template matching techniques in computer vision: theory and practice*. John Wiley & Sons, 2009.

[12] Zhengyou Zhang. Determining the epipolar geometry and its uncertainty: A review. *International Journal of Computer Vision*, 27:161–195, 1998.

[13] Zhengyou Zhang, Rachid Deriche, Olivier Faugeras, and Quang-Tuan Luong. A robust technique for matching two uncalibrated images through the recovery of the unknown epipolar geometry. *Artificial intelligence*, 78(1-2):87–119, 1995.

[14] Tobias Wissel, Benjamin Wagner, Patrick Stüber, Achim Schweikard, and Floris Ernst. Data-driven learning for calibrating galvanometric laser scanners. *IEEE Sensors Journal*, 15(10):5709–5717, 2015.

[15] Qing Li, Mengjuan Chen, Qingyi Gu, and Idaku Ishii. A flexible calibration algorithm for high-speed bionic vision system based on galvanometer. In *2022 IEEE/RSJ International Conference on Intelligent Robots and Systems (IROS)*, pages 4222–4227. IEEE, 2022.